Karaj branch

Journal of Applied Chemical Research
jacr.kiau.ac.ir

Journal of Applied Chemical Research, 13, 1, 8-23 (2019)

Preparation and Application of $Fe_3O_4@SiO_2@OSO_3H$ Nanocomposite as a Green Catalyst for the Synthesis of Octahydroquinazolinones

Mohammad Ali Ghasemzadeh

Department of Chemistry,Qom Branch, Islamic Azad University, Qom, Iran

(Received 25 May 2018; Final revised received 28 Aug. 2018)

Abstract

In this research the magnetite nanoparticles supported silica sulfonic acid ($Fe_3O_4@SiO_2@OSO_3H$) was used as a green and efficient catalyst for the preparation of octahydroquinazolinone derivatives as biologically active heterocyclic compounds. This procedure avoids hazardous reagents, solvents, catalyst and can be an eco-friendly alternative to the existing methods. The one-pot three-component reaction of aldehydes, dimedone and urea or thiourea has several advantages such as: simple procedure, eco-friendly approach, excellent yields, short reaction times, little catalyst loading, simple purification and facile catalyst separation. In addition, the synthesis and application of $Fe_3O_4@SiO_2@OSO_3H$ nanocomposite as a robust and recoverable heterogeneous nanocatalyst is described. Fe_3O_4 nanoparticles encapsulated-silica particles bearing sulfonic acid were readily recovered using an external magnet and could be reused several times without significant loss of its reactivity. The catalyst was fully characterized by different spectroscopic techniques including VSM, FT-IR, SEM, XRD, EDX and TEM analysis.

Keywords: *$Fe_3O_4@SiO_2@OSO_3H$, Nanoparticles, Multi-component reaction, Core–shell, Octahydroquinazolinone.*

[*]***Corresponding author****: Mohammad Ali Ghasemzadeh,Department of Chemistry, Qom Branch, Islamic Azad University, Qom, Iran, E-mail: E-mail: ghasemzadeh@qom-iau.ac.ir.*

Introduction

In recent years, to decrease waste and atom economy in the using raw materials, the aim of technology and science has been shifting toward more environment friendly, reusable catalysts and sustainable resources [1]. Recently, magnetite nanoparticles (MNPs) have been intensively studied because of their broad applications such as ferro fluids, digital media recording and targeted drug delivery [2,3]. Moreover, the coated magnetite nanoparticles have several uses in chemotherapeutics, magnetic hyperthermia, magnetic resonance imaging, etc. [4,5]. However, bare Fe_3O_4 NPs tend to aggregate into large clusters, have an easy oxidation in air, dispersion, loss of magnetism and agglomeration because of their high specific area and strong inter particle interaction, which limit their usage. In this regard, great attention has recently been paid to the preparation of the amorphous silica layer is a hopeful and significant approach in the expansion of magnetite nanoparticles for both basic study and technological applications [6]. Silica shell in nanocomposite is chemically inert and has high stability versus aggregation. Furthermore, the presence of silanol moieties on the surface can readily be functionalized through the suitable surface modifications, enabling the introduction of a variety of various functionalities [7]. Therefore, the outer shell of silica not only protects the inner magnetite core from oxidation but also provides sites for surface functionalization using various groups such as amino-silane [8], proline [9], sulfamic acid [10] and sulfonic acid [11].

In recent years, nano-Fe_3O_4 encapsulated-silica particles bearing sulfonic acid (Fe_3O_4@SiO_2@OSO_3H) nanoparticles were used as an active catalyst in the synthesis of 1,8-dioxo-octahydroxanthene [12], indazolo[2,1-b]phthalazine-triones and pyrazolo[1,2-b]phthalazine-diones [13], functionalized pyrimido[4,5-b]quinolines and indeno fused pyrido[2,3-d]pyrimidines [14] and 3,4-dihydropyrimidinones/thiones [15].

Multi-component reactions are assuming an increasingly important role in organic and medicinal chemistry owing to their high atom economy, simple methods, and excellent yields. They can be applied to fabricate new heterocyclic compounds with a diversity of biological activities, and have become an important means of heterocyclic synthesis [16,17]. The advantages of multicomponent reactions are significantly expanded if they are conducted with green procedures. In recent years, in order to decrease waste and the use of raw materials, the aim of science and technology has been shifting toward more environment friendly, sustainable resources and reusable catalysts [18].

Recently, the syntheses of octahydroquinazolinones have relieved great interest in the organic synthesis because of their potential antibacterial activity against *Staphylococcus aureus*, *Escherichia coli*, and *Pseudomonas aeruginosa* [19]. In addition they have showed calcium antagonist activity [20].

The three-component reaction of aldehydes, dimedone and urea/thiourea has been reported using MCRs in the presence of diverse catalysts including SiO_2-$NaHSO_4$ [21], [tbmim]Cl_2/$AlCl_3$ [22], silica sulfuric acid [23], thiamine hydrochloride [24], $ZrOCl_2.8H_2O$ [25], HCl [26], and H_2SO_4 [27].

The aim of this approach is to highlight the synergistic effects of the combined use of multicomponent coupling reactions and application of solid Bronsted acid catalyst supported on nanostructure materials with inherent magnetic property for the development of new eco-compatible strategy for heterocyclic synthesis. Therefore, in the continue of our interest on sustainable approaches in the preparation of organic compounds using nanocatalysts [28-33], herein we report a straightforward method for the one-pot synthesis of octahydroquinazolinone in the presence of Fe_3O_4@silica sulfonic acid as an proficient, mild and recyclable catalyst (Scheme1).

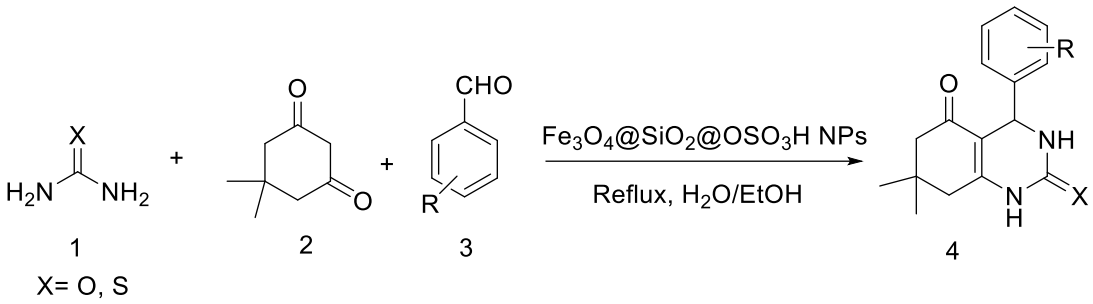

Scheme 1. Fe_3O_4@SiO_2@OSO_3H NPs catalyzed synthesis of octahydroquinazolinones.

Experimental

Materials and Methods

Chemicals were purchased from the Sigma-Aldrich and Merck in high purity. All melting points are uncorrected and were determined in capillary tube on Boetius melting point microscope.^{1}H NMR and ^{13}C NMR spectra were obtained on Bruker 400 MHz spectrometer with DMSO-d_6 as solvent using TMS as an internal standard. FT-IR spectrum was recorded on Magna-IR, spectrometer 550. The elemental analyses (C, H, N) were obtained from a

Carlo ERBA Model EA 1108 analyzer. Powder X-ray diffraction (XRD) was carried out on a Philips diffractometer of X'pert Company with mono chromatized Cu Kα radiation (λ = 1.5406 Å). Microscopic morphology of products was visualized by SEM (LEO 1455VP). The mass spectra were recorded on a Joel D-30 instrument at an ionization potential of 70 eV. Transmission electron microscopy (TEM) was performed with a Jeol JEM-2100UHR, operated at 200 kV. Magnetic properties were obtained on a BHV-55 vibrating sample magnetometer (VSM) made by MDK-I.R.Iran. The compositional analysis was done by energy dispersive analysis of X-ray (EDX, Kevex, Delta Class I).

Preparation of Fe_3O_4 nanoparticles

Fe_3O_4 nanoparticles were prepared according to the procedure reported by Zhang et al [34]. To a solution of $FeCl_2.4H_2O$ (2.5 g) and $FeCl_3.6H_2O$ (6 g) in 30 mL deionized water was added dropwise 1.0 mL of concentrated hydrochloric acid at room temperature. The solution was added in to 300 mL of 1.5 mol L^{-1} NaOH and then the solution was stirred vigorously at 80 °C until precipitation. Afterwards, the prepared magnetic nanoparticles were separated magnetically, washed with deionized water and then dried at 70 °C for 8 h.

Preparation of Fe_3O_4@SiO_2 nanocomposite

The core-shell Fe_3O_4@SiO_2 microspheres were prepared according to the previously reported method [35]. Briefly 1g of Fe_3O_4 nanoparticles were treated with 0.5 M HCl aqueous solution (25 mL) by sonication. After treatment for 10 min, the magnetite particles were separated and washed with deionized water, and then homogeneously dispersed in the mixture of ethanol (60 mL), deionized water (100 mL) and concentrated ammonia aqueous solution (10 mL, 28 wt.%), followed by the addition of tetraethylorthosilicate (TEOS, 0.22 g, 0.144 mmol). After stirring at room temperature for 2 h, the Fe_3O_4@SiO_2 microspheres were separated using an external magnet and washed with ethanol and water.

Preparation of Fe_3O_4@SiO_2@OSO_3H nanocomposite

Fe_3O_4@SiO_2@OSO_3H MNPs were prepared according to a previously reported procedure by Kiasat and Davarpanah (Scheme 2) [13]. A suction flask equipped with a constant-pressure dropping funnel. The gas outlet was connected to a vacuum system through an adsorbing solution of alkali trap. Firstly, Fe_3O_4@Silica (1 g) was added to the flask and dispersed in dry CH_2Cl_2 (10 mL) by ultrasonic for 30 min. Subsequently, chlorosulfonic acid (1 ml) was added drop-wise to a cooled (ice-bath) solution of Fe_3O_4@SiO_2 (1 g) over a period of 30 min

at room temperature. After completion of the addition, the mixture was stirred for a further 6 h until to allow for the complete dissipation of HCl from the reaction vessel. The resulted MNPs were separated using an external magnet and washed with ethanoland water before being dried in an oven at 70°C to give Fe_3O_4@SiO_2@OSO_3H as a brown powder.

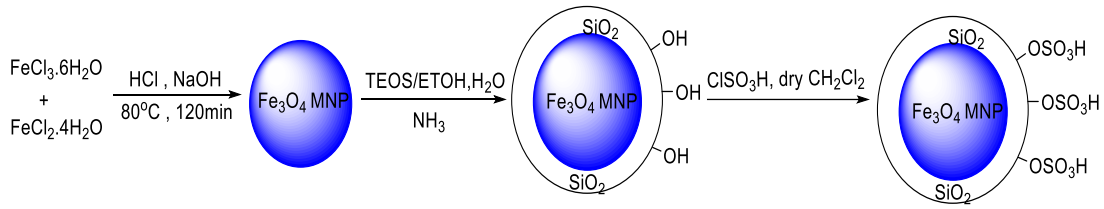

Scheme 2. Preparation steps of sulfonic acid-functionalized magnetic Fe_3O_4 nanoparticles.

*General procedure for the synthesis of octahydroquinazolinones (**4a-4t**)*

A mixture of aldehyde (1mmol), dimedone (1 mmol), urea/thiourea (1mmol) and Fe_3O_4@SiO_2@OSO_3H (0.01 g, 3 mol%) was taken in a round bottom flask and the mixture was refluxed using 2.5 mL ethanol and 2.5 mL of water.Progress of the reaction was continuously monitored by TLC. When the reaction was completed, the mixture was cooled to the room temperature and then the residue was dissolved in methanol and the nanocatalyst was separated using an external magnet. The solvent was evaporated under vacuum and the solid obtained was washed several times with dichloromethane to afford the pure octahydroquinazolinones.

All of the products were characterized and identified with m.p., ^{1}H NMR, ^{13}C NMR and FT-IR spectroscopy techniques. Spectral data of the new products are given below.

4-(4-cyanophenyl)-7,7-dimethyl-1,2,3,4,5,6,7,8-octahydroquinazoline-2,5-dione **(4l)**

White solid; m.p. 226-228 °C. ^{1}H NMR (400 MHz, DMSO-d_6): δ= 0.90 (s, 3H, CH_3), 1.01 (s, 3H, CH_3), 2.07 (d, 1H, CH_2), 2.15-2.36 (m, 2H, CH_2), 2.48 (s, 1H, CH_2), 5.26 (s, 1H, CH), 7.23-7.29 (m, 4H, ArH), 7.73 (bs, 1H, NH), 9.49 (bs, 1H, NH). ^{13}C NMR (100 MHz, DMSO-d_6): δ= 28.4, 30.3, 33.8, 51.3, 53.1, 109.1, 116.3, 126.8, 127.8, 138.3, 142.9, 153.3, 153.8, 190.3. FT-IR (KBr): 3387, 3182, 2944, 2198, 1698, 1623, 1375 cm^{-1}. MS (EI) (*m/z*): 295 (M^+). Anal. calcd For: $C_{17}H_{17}N_3O_2$: C 69.14, H 5.80, N 14.23. Found: C 69.23, H 5.86, N 14.19.

4-(7,7-dimethyl-2,5-dioxo-1,2,3,4,5,6,7,8-octahydroquinazolin-4-yl)benzaldehyde **(4m)**

White solid; m.p. 216-217 ºC. ^{1}H NMR (400 MHz, DMSO-d_6): δ= 0.92 (s, 3H, CH_3), 1.00 (s, 3H, CH_3), 2.97 (d, 1H, CH_2), 2.12 (d, 1H, CH_2), 2.31 (d, 1H, CH_2), 2.43 (d, 1H, CH_2), 5.66 (s, 1H, CH), 7.32-7.39 (m, 4H, ArH), 7.74 (bs, 1H, NH), 8.18 (s, 1H, CHO), 9.57 (bs, 1H, NH). ^{13}C NMR (100 MHz, DMSO-d_6): δ= 27.1, 30.2, 33.8, 52.5, 54.1, 116.8, 127.1, 127.8, 139.9, 141.4, 152.4, 153.7, 194.1, 203.5. FT-IR (KBr): 3363, 3156, 2956, 1702, 1618, 1364 cm^{-1}. MS (EI) (*m/z*): 300 (M^+). Anal. calcd for $C_{17}H_{18}N_2O_3$: C 68.44, H 6.08, N 9.39. Found: C 68.31, H 6.19, N 9.45.

4-(4-(methylthio)phenyl)-7,7-dimethyl-1,2,3,4,5,6,7,8-octahydroquinazoline-2,5-dione **(4n)**
White solid; m.p. 238-239 ºC. ^{1}H NMR (400 MHz, DMSO-d_6): δ= 0.87 (s, 3H, CH_3), 0.99 (s, 3H, CH_3), 2.01 (d, 1H, CH_2), 2.15-2.26 (m, 2H, CH_2), 2.36 (s, 1H, CH_2), 2.41 (s, 3H, SCH_3), 5.09 (s, 1H, CH), 7.13-7.19 (m, 4H, ArH), 7.73 (bs, 1H, NH), 9.45 (bs, 1H, NH). ^{13}C NMR (100 MHz, DMSO-d_6): δ= 16.3, 28.4, 30.3, 33.8, 51.3, 53.1, 108.8, 127.4, 128.4, 138.3, 142.9, 153.4, 153.9, 195.2. FT-IR (KBr): 3279, 3145, 2923, 1693, 1611, 1351 cm^{-1}. MS (EI) (*m/z*): 316 (M^+). Anal. calcd for $C_{17}H_{20}N_2O_2S$: C 64.53, H 6.37, N 8.85. Found: C 64.65, H 6.44, N 8.72.

Results and discussion

Characterization of the Fe_3O_4@SiO_2@OSO_3H NPs as a solid acid catalyst

In the preliminary experiments Fe_3O_4@silica sulfonic acid nanostructures was prepared and characterized by EDX, SEM, XRD, FT-IR, VSM and TEM analysis.

The chemical purity of the samples as well as their stoichiometry was tested by EDX studies. The EDX spectrum given in Figure 1a shows the presence of Fe and O as the only elementary components of Fe_3O_4 NPs. EDX spectrum of Fe_3O_4@SiO_2 (Figure 1b) shows the elemental compositions are (Fe, O and Si) of core-shell nanoparticles. The EDX spectrum of Fe_3O_4@SiO_2@OSO_3H (Figure 1c) shows the elemental compositions are (Fe, Si, O and S) of magnetic nanocomposite.

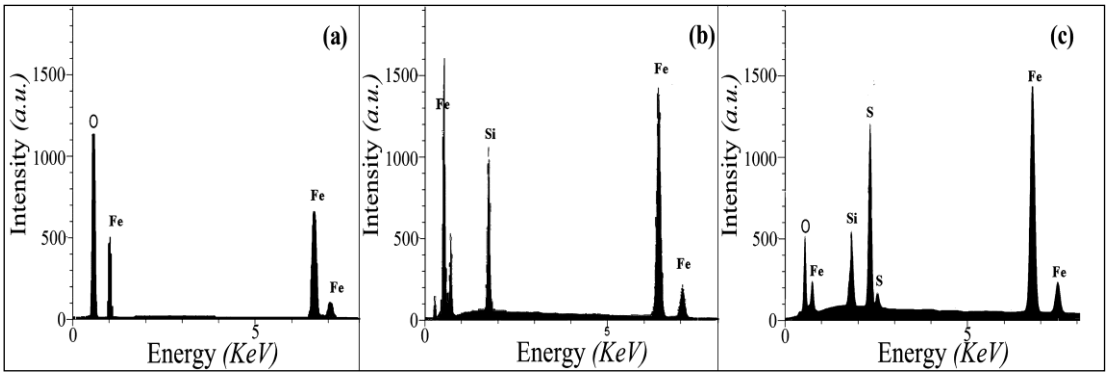

Figure 1. EDX spectra of (a) Fe_3O_4, (b) $Fe_3O_4@SiO_2$ and (c) $Fe_3O_4@SiO_2@OSO_3H$ MNPs**.**

Scanning electron microscopy (SEM) is a useful tool for determining the size distribution, particles shape, and porosity. It has been a primary tool for characterizing the surface morphology and fundamental physical properties of the surface. According to Figure 2b, $Fe_3O_4@SiO_2$ nanoparticles still keep the morphological properties of Fe_3O_4 (Figure 2a) except for a slightly larger particle size and smoother surface, while silica are uniformly coated on the Fe_3O_4 particles to form silica shell compared to the $Fe_3O_4@SiO_2$, The SEM image shown in Figure 2c demonstrates that $Fe_3O_4@SiO_2@OSO_3H$ nanoparticles are nearly spherical with about 30 nm in size.

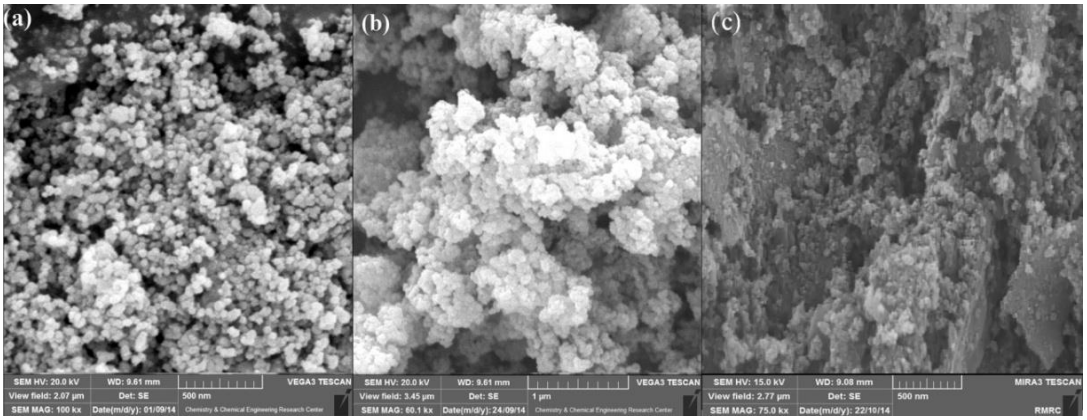

Figure 2. SEM images of (a) Fe_3O_4, (b) $Fe_3O_4@SiO_2$ and (c) $Fe_3O_4@SiO_2@OSO_3H$ MNPs.

The structure of Fe_3O_4 (a), $Fe_3O_4@SiO_2$ (b) and Fe_3O_4@silica sulfonic acid (c) were analyzed by X-ray diffraction (XRD) spectroscopy (Figure 3). XRD diagram of the bare Fe_3O_4 NPs displayed patterns consistent with the patterns of spinel ferrites described in the literature (Figure 3) [10]. The same peaks were observed in the both of the $Fe_3O_4@SiO_2$ and Fe_3O_4@silica sulfuric acid XRD patterns, indicating retention of the crystalline spinel ferrite

core structure during the silica-coating process. The average MNPs core diameter of Fe_3O_4, Fe_3O_4@SiO_2 and Fe_3O_4@silica sulfonic acid were calculated to be about 18, 25 and 32 nm, respectively from the XRD results by Scherrer's equation.

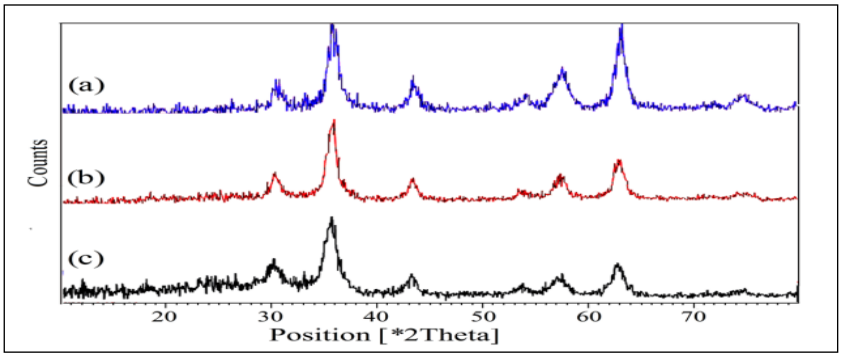

Figure 3. XRD patterns of (a) Fe_3O_4, (b) Fe_3O_4@SiO_2 and (c) Fe_3O_4@SiO_2@OSO_3H MNPs.

The FT-IR spectra of Fe_3O_4 nanoparticles (Figure 4a), Fe_3O_4@SiO_2 (Figure 4b), and Fe_3O_4@silica sulfonic (Figure 4c) acid are shown in Figure 4. The FT-IR analysis of the Fe_3O_4@SiO_2 and Fe_3O_4@silica sulfonic acid exhibits two basic characteristic peaks at ~3300 cm^{-1} (O–H stretching) and 580 cm^{-1} (Fe–O vibration) [36]. The band at 1081 cm^{-1} comes from the Si–O–Si group. The presence of saulfonyl group in Fe_3O_4@silica sulfonic acid is confirmed by 1217 cm^{-1} and 1124 cm^{-1} bands, which were covered by a stronger absorption of Si–O bonds at 1081 cm^{-1}[10]. A wide bond at 2500-3409 cm^{-1} is due to the stretching of OH groups in the SO_3H.

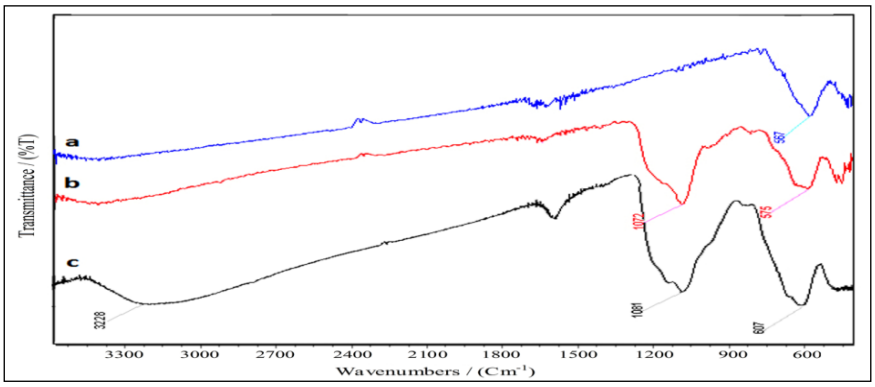

Figure 4.FT-IR spectra of (a) Fe_3O_4, (b) Fe_3O_4@SiO_2 and (c) Fe_3O_4@SiO_2@OSO_3H MNPs.

The magnetic properties of the uncoated magnetic iron oxide (Fe_3O_4), Fe_3O_4@SiO_2, and Fe_3O_4@SiO_2-SO_3H were measured by vibrating sample magnetometer, VSM, at room temperature (Figure 5). In Figure 5, the hysteresis loops that are characteristic of

superparamagnetic behavior can be clearly observed for all the nanoparticles. Superparamagnetism is the responsiveness to an applied magnetic field without retaining any magnetism after removal of the applied magnetic field. From M versus H curves, the saturation magnetization value (Ms) of uncoated Fe_3O_4 NPs was found to be 48.12 emu g^{-1} (Figure 5a). For $Fe_3O_4@SiO_2$ (Figure 5b) and $Fe_3O_4@SiO_2@OSO_3H$ (Figure 5c), the magnetization obtained at the same field were 40.16 and 35.82 emu g^{-1}, respectively, lower than that of uncoated Fe_3O_4. These results indicated that the magnetization of Fe_3O_4 decreased considerably with the increase of SiO_2 and SO_3H. This is mainly attributed to the existence of nonmagnetic materials on the surface of the nanoparticles.

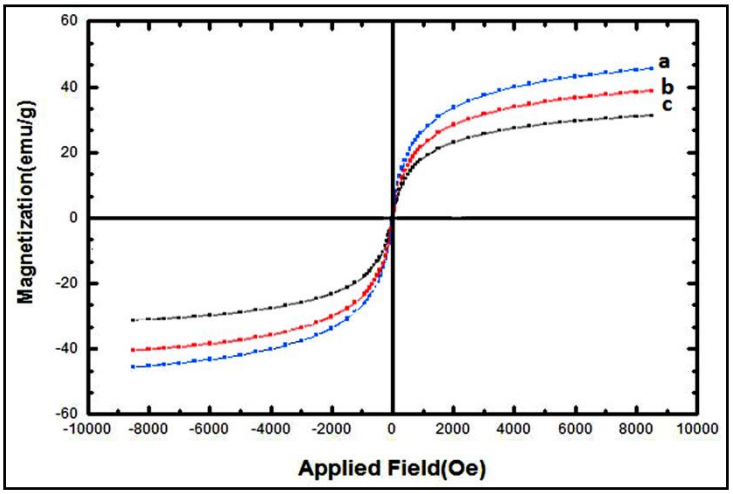

Figure 5.VSM magnetization curves of the (a) Fe_3O_4, (b) $Fe_3O_4@SiO_2$ and (c) $Fe_3O_4@SiO_2@OSO_3H$ MNPs.

The size and morphology of $Fe_3O_4@SiO_2@OSO_3H$ nanoparticles were analyzed by Transmission electron microscopy (TEM) (Figure 6). The results show that these nanocatalysts consist of spherical particles with the crystallite size about 30 nm, confirming the results calculated from Scherrer's formula based on the XRD pattern.

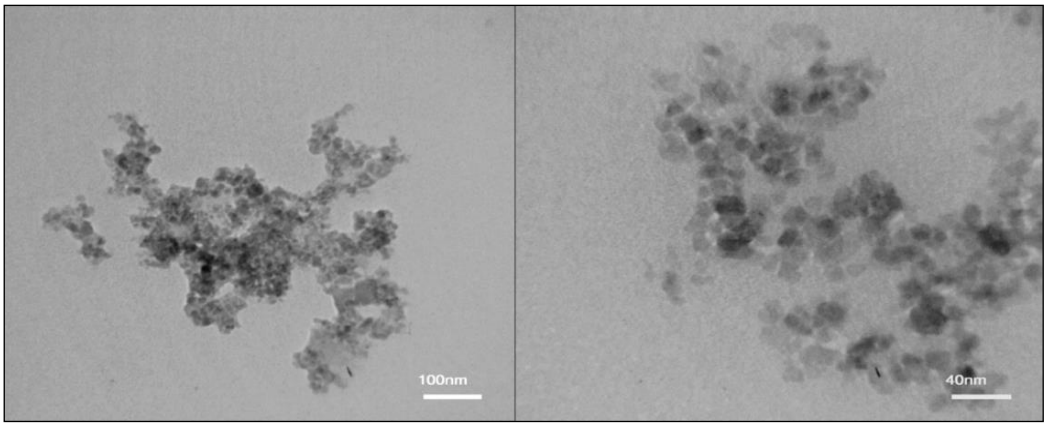

Figure 6.TEM images of $Fe_3O_4@SiO_2@OSO_3H$ nanocomposite.

In this research, in order to determine the optimized reaction conditions, the reaction of urea 1, dimedone 2 and 4-nitrobenzaldehyde 3c was selected as model study and the reaction conditions were optimized on the basis of solvent, catalyst and different temperatures (Scheme 3).

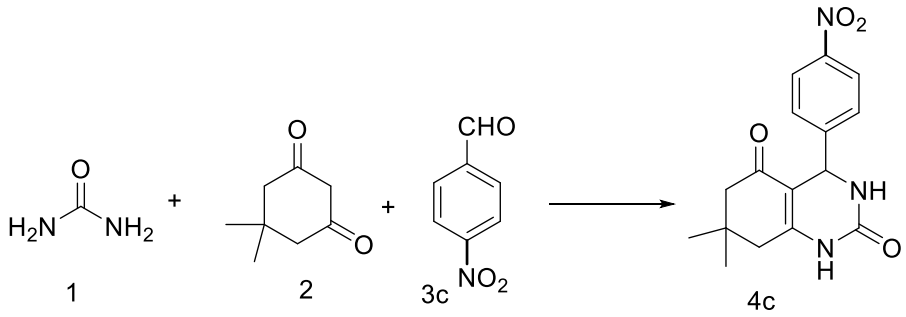

Scheme 3.The model reaction for the synthesis of octahydroquinazoline 4c**.**

The influence of solvent was studied when the model reaction was performed using $Fe_3O_4@SiO_2@OSO_3H$ NPs nanoparticles under various solvents and also solvent-free conditions in different temperatures (Table 1). The best results were obtained under reflux conditions regarding reaction time and yield of the corresponding product (Table1, Entries 4-10). Moreover, Table 1 shows that, the solvent has a great effect on the accelerating of the reaction. The best results (97% yield, 60 min) were obtained in water/ethanol under reflux conditions for this multi-component reaction (Table 1, Entry 4). The significant results presented in Table 1 are related to the hydrogen bonding between water/ethanol and substrates that promote the nucleophilic attack of the reactants.

Table 1. Synthesis of 4-(4-nitrophenyl)-7,7-dimethyl-1,2,3,4,5,6,7,8 octahydroquinazoline-2,5-dione (4c) in different solvents.[a]

Entry	Solvent	T/°C	Time (min)	Yield (%)[b]
1	Solvent-free	25	180	trace
2	Solvent-free	100	120	25
3	Water/EtOH	25	120	40
4	**Water/EtOH**	**Reflux**	**60**	**97**
5	EtOH	Reflux	80	70
6	Water	Reflux	90	65
7	CH_3CN	Reflux	120	52
8	DMF	Reflux	120	44
9	CH_2Cl_2	Reflux	180	25
10	Toluene	Reflux	180	36

[a] Reaction conditions: 4-nitrobenzaldehyde (1 mmol), (1mmol), urea (1mmol)and $Fe_3O_4@SiO_2@OSO_3H$ NPs (0.01 g). [b] Isolated Yields

Afterward, to show the merit of the present approach in comparison with other catalysts the model reaction were investigated in the absence and also in the presence of various catalysts for the synthesis of octahydroquinazoline (4c) (Table 2). In a control experiment, when the reaction was performed without the catalyst only a trace amount of the product was observed, confirming that the presence of the catalyst is necessary for the three-component reaction of urea, dimedone and 4-nitrobenzaldehyde. Then, to test the efficiency of the catalytic activity, we choose to focus our initial studies using various nanocatalysts including AgI, CuO, CaO, Co_3O_4, MgO, SiO_2, $Fe_3O_4@SiO_2$, and $Fe_3O_4@SiO_2@OSO_3H$ in H_2O/EtOH under reflux conditions (Table 2). From the results provided in Table 2, it was clear that $Fe_3O_4@SiO_2$-OSO_3H afforded the corresponding octahydroquinazoline 4c in excellent yield and short reaction time (60 min, 97 % yield).

Table 2. Synthesis of octahydroquinazoline 4c using various catalysts[a].

Entry	Catalyst	Catalyst loading (g)	Time (min)	Yield (%)[b]
1	None	-	180	trace
2	AgI	0.05	120	55
3	CuO	0.05	110	60
4	CaO	0.05	150	35
5	Co_3O_4	0.05	100	65
6	MgO	0.05	140	25
7	SiO_2	0.05	90	55
8	$Fe_3O_4@SiO_2$	0.05	75	70
9	$Fe_3O_4@SiO_2@SO_3H$	0.05	60	97
10	$Fe_3O_4@SiO_2@SO_3H$	0.03	60	97
11	**$Fe_3O_4@SiO_2@SO_3H$**	**0.01**	**60**	**97**
12	$Fe_3O_4@SiO_2@SO_3H$	0.005	85	70

[a] Water/ethanol as solvent under reflux conditions.[b] Isolated Yields

The greater catalytic activity of $Fe_3O_4@SiO_2@OSO_3H$ in comparison with other nanocatalysts is related to the SO_3H groups on the surfaces of the catalyst, which could provide efficient acidic sites. The reaction was also investigated with different catalyst loading, revealing that 0.01 g (3 mol%) of the catalyst provided the best results in terms of reaction time, economy of catalyst charge, and reaction yield (Table 2, entry 11). As shown in Table 2 increasing the amount of catalyst does not improve the yield of the product any further, whereas decreasing the amount of catalyst leads to decrease in the product yield. Hence, the optimum concentration of $Fe_3O_4@SiO_2@OSO_3H$ was chosen 0.01 g in the model reaction.

After optimization of the reaction conditions, we used a diversity of aldehydes to investigate three-component reactions in the presence of $Fe_3O_4@SiO_2@OSO_3H$ NPs under reflux conditions (Table 3). We observed that various aryl aldehydes could be introduced in high efficiency and produced high yields of products in high purity. The data of Table 3 show that sterically hindered aromatic aldehydes required longer reaction times in comparison with *p*-substituted aryl aldehydes. In addition, aromatic aldehydes bearing electron-withdrawing groups such as Cl, Br, and NO_2 in the *p*-position reacted very smoothly while reactants with electron-releasing groups such as methoxy and isopropyl decreased both the rate of the reaction and the yield of corresponding product (Table 3).

Table 3. One-pot synthesis of octahydroquinazolinones (4a-t) catalyzed by $Fe_3O_4@SiO_2@OSO_3H$ MNPs. [a]

Entry	Adehyde (R)	X	Product	Time (min)	Yield,[b](%)	m.p.ºC (Lit. m.p.ºC)
1	H	O	4a	80	92	289-290 (290-292) [22]
2	4-Cl	O	4b	65	97	309-311 (> 300) [22]
3	4-NO_2	O	4c	60	97	303-305 (302-304) [22]
4	3-NO_2	O	4d	70	93	297-298 (298-300) [22]
5	4-F	O	4e	65	94	135-137 (134-136) [22]
6	4-Br	O	4f	70	95	320-322 (234-326) [25]
7	3-Cl	O	4g	70	92	278-280 (280-282) [22]
8	4-CH_3	O	4h	85	90	303-304 (300-302) [25]
9	4-OCH_3	O	4i	95	88	281-283 (278-280) [21]
10	2-Cl	O	4j	100	92	274-275 (271-273) [25]
11	2-OH	O	4k	110	86	184-185 (184-186) [21]
12	4-CN	O	4l	65	94	226-228

13	4-CHO	O	4m	70	95	216-217
14	4-SCH_3	O	4n	80	90	238-239
15	H	S	4o	90	90	281-282 (283-285) [22]
16	4-Cl	S	4p	75	94	218-220 (219-221) [27]
17	3-Cl	S	4q	80	90	274-276 (275-277) [22]
18	4-CH_3	S	4r	95	85	284-285 (280-282) [25]
19	4-OCH_3	S	4s	100	84	271-272 (273-284) [22]
20	4-Br	S	4t	85	90	285-286 (285-287) [22]

[a]Reaction conditions: aldehyde (1 mmol), dimedone(1mmol), urea/thiourea (1mmol) and Fe_3O_4@SiO_2@SO_3H NPs (0.01 g) in H_2O/EtOH under reflux conditions. [b]Isolated Yields

A plausible mechanism for the synthesis of octahydroquinazolinones using Fe_3O_4@SiO_2@OSO_3H NPs has been shown in Scheme 4. It is likely that Fe_3O_4@SiO_2@OSO_3H as a Bronsted acid which increases the electrophilicity of the carbonyl groups of the dimedone and aldehyde by means of a strong coordinate bond. The first step is believed to be a Knoevenagel condensation between the aldehyde and dimedone to generate adduct A, which acts as a Michael acceptor. Then urea/thiourea attacks to intermediate A in a Michael-type reaction to produce an open chain intermediate B which convert to intermediate C. Finaly intermediate C undergoes intramolecular cyclization by the nucleophilic attack of NH_2 to carbonyl group followed by dehydration to produce octahydroquinazolinon.

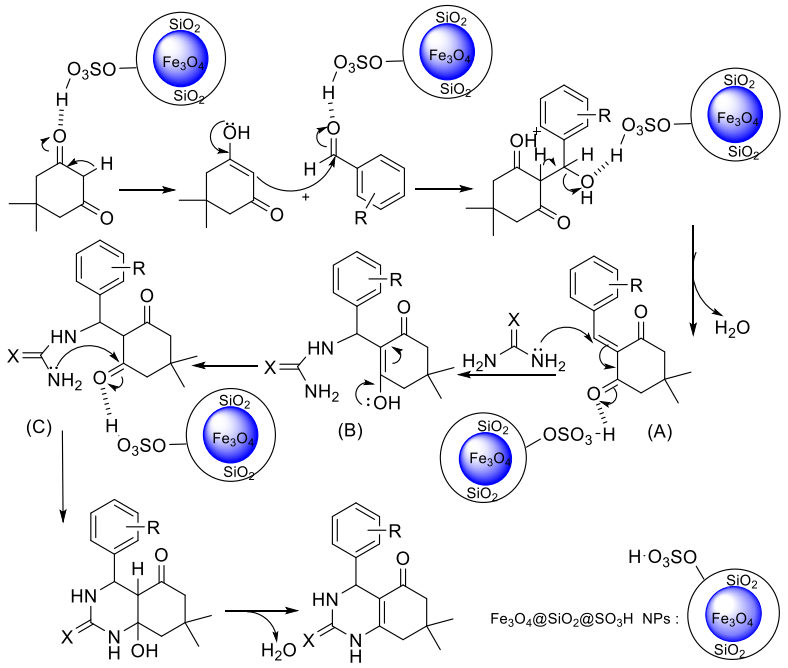

Scheme 4. The proposed mechanism for the synthesis of octahydroquinazolinones.

Recycling and Reusing of the Catalyst

When the reaction was complete, the formed product was dissolved in methanol and then the nanocatalyst was easily separated using an external magnet. The recovered nanoparticles were washed several times with methanol and ethylacetate and then dried at 60 ^{o}C for 10 h. To investigate lifetime and level of recoverability of the $Fe_3O_4@SiO_2@OSO_3H$ NPs, the model study was carried out several times by use of recycled magnetite nanoparticles. We observed that the recovered magnetite nanoparticles could be used for five successive runs with a slightly decreased in activity as indicated in Table 4.

Table 4. Reusability of the $Fe_3O_4@SiO_2@OSO_3H$ nanocomposite.

Yield (%)				
First	**Second**	**Third**	**Fourth**	**Fifth**
97	95	92	90	87

Conclusion

In conclusion, a novel and highly effective approach for the synthesis of octahydroquinazoline derivatives by treatment of urea/thiourea, dimedone and aromatic aldehydes has been developed in the presence of $Fe_3O_4@SiO_2@OSO_3H$ nanoparticles as catalyst. The present method is mild, easy, efficient and eco-friendly which provided octahydroquinazolines in excellent yields and short reaction times. The one-pot nature and the use of heterogeneous solid Bronsted acid as an eco-friendly catalyst make it an interesting alternative to multi-step approaches.

Acknowledgements

The authors thank the Islamic Azad University, Qom Branch, Qom, I. R. Iran for supporting this work [grant number 2014-13929].

References

[1] Y. Zhang, Y. Zhao, C. Xia, *J. Mol. Catal. A: Chem*., 306, 107 (2009).

[2] K. Raj, R. Moskowitz, *J. Magn. Magn. Mater*., 85, 233 (1990).

[3] Q.A. Pankhurst, J. Connolly, S.K. Jones J. Dobson, *J. Phys. D Appl. Phys*., 36, R167 (2003).

[4] M.L. McCormick, E.J. Bouwer, P. Adriaens, *Environ. Sci. Technol*., 36, 403 (2002).

[5] P.I. Girginova, A.L. Daniel-da-Silva, C.B. Lopes, P. Figueira, M. Otero, V.S. Amaral, E. Pereira, T. Trindade, *J. Colloid Interface Sci*. 345, 234 (2010).

[6] A. Farhadi, M.A. Takassi, M. Enjilzadeh, F. Davod, *J. Appl. Chem. Res*., 12, 48 (2018).

[7] J. Davarpanah, A.R. Kiasat, S. Noorizadeh, M. Ghahremani, *J. Mol. Catal. A: Chem*., 376, 78 (2013).

[8] J. Safari, Z. Zarnegar, *J. Mol. Struc*., 1072, 53 (2014).

[9] H. Yang, S. Li, X. Wang, F. Zhang, X. Zhong, Z. Dong, J. Ma, *J. Mol. Catal. A: Chem*., 363-364, 404 (2012).

[10] M.Z. Kassaee, H. Masrouri, F. Movahedi, *Appl. Catal. A: Gen*., 395, 28 (2011).

[11] F. Nemati, M.M. Heravi, R. Saeedirad, *Chin. J. Catal*., 33, 1825 (2012).

[12] H. Naeimi, Z.S. Nazifi, *J. Nanopart. Res*., 15, 2026 (2013).

[13] A. R. Kiasat, J. Davarpanah, *J. Mol. Catal. A: Chem*., 373, 46 (2013).

[14] F. Nemati R. Saeedirad, *Chin. Chem. Lett*., 24, 370 (2013).

[15] A.R. Kiasat, J. Davarpanah, *Res. Chem. Intermed*., 41, 2991 (2015).

[16] M. Mahdipour, H. Khabazzadeh, E. Tavakolinejad Kermani, *J. Sci. I. R. Iran.*, 27, 119 (2016).

[17] M.S. Singh, S. Chowdhury, *RSC Adv*., 2, 4547 (2012).

[18] A. Domling, I. Ugi, *Angew. Chem. Int. Ed*. 39, 3168 (2000).

[19] M. Kidwai, S. Saxena, M.K.R. Khan, S. Thukral, *Eur. J. Med. Chem*., 40, 816 (2005).

[20] M. Yarim, S. Sarac, F.S. Kilic, K. Erol, *Farmaco*., 58, 17 (2003).

[21] S.H.S. Azzam, A. Siddekha, A. Nizam, M.A. Pasha, *Chin. J. Catal*., 33, 677 (2012).

[22] K.S. Niralwad, B.B. Shingate M.S. Shingare, *J. Chin. Chem. Soc.*, 57, 89 (2010).

[23] A. Mobinikhaledi, N. Foroughifar, H. Khodaei, *Eur. J. Chem*. 4, 291 (2010).

[24] P.V. Badadhe, A.V. Chate, D.G. Hingane, P.S. Mahajan, N.M. Chavhan, C.H. Gill, *J. Korean Chem. Soc*., 55, 936 (2011).

[25] S. Karami, B. Karami, S. Khodabakhshi, *J. Chin. Chem. Soc*., 60, 22 (2013).

[26] P. Shanmugam, C. Sabastein, P.T. Perumal, *Ind. J. Chem.*, 43B, 674 (2004).

[27] Z. Hassani, M.R. Islami, M. Kalantari, *Bioorg. Med. Chem. Lett*., 16, 4479 (2006).

[28] M.A. Ghasemzadeh, J. Safaei-Ghomi, H. Molaei, *C. R. Chimie*., 15, 969 (2012).

[29] M.A. Ghasemzadeh, N. Ghasemi-Seresht, *Res. Chem. Intermed*., 41, 8625 (2015).

[30] M.A. Ghasemzadeh, J. Safaei-Ghomi, *J. Chem. Res*., 38, 313 (2014).

[31] B. Mirhosseini-Eshkevari, M.A. Ghasemzadeh, J. Safaei-Ghomi, *Res. Chem. Intermed*., 41, 7703 (2015).

[32] M.A. Ghasemzadeh, B. Mirhosseini-Eshkevari, M.H. Abdollahi-Basir, *Comb. Chem. High. T. Scr*., 19, 592 (2016).

[33] M.A. Ghasemzadeh, *Acta. Chim. Slov*., 62, 977, (2015).

[34] H. Lu, Y. Yang, S.H. Deng, J. Zhang, Z.H. *Aust. J. Chem.*, 63, 1290 (2010).

[35] X.Q. Xu, C.H. Deng, M.X. Gao, W.J. Yu, P.Y. Yang, X. M. Zhang, *Adv. Mater.*, 18, 3289 (2006).

[36] Y. Lin, H. Chen, K. Lin, B. Chen, C. Chiou, *J. Environ. Sci*., 23, 44 (2010).